Anisotropic Gelation Seeded by a Rod-Like Polyelectrolyte

Yukari Shigekura,[†] Hidemitsu Furukawa,[†] Wei Yang,[†] Yong Mei Chen,[†,‡] Tatsuo Kaneko,[§] Yoshihito Osada,[†] and Jian Ping Gong*[,†,||]

Division of Biological Sciences, Graduate School of Science, Hokkaido University, Sapporo 060-0810, Japan, Creative Research Initiative "SOUSEI" , Hokkaido University, Sapporo 001-0021, Japan, School of Materials Science, Japan Advanced Institute of Science and Technology, Ishikawa 923-1292, Japan, and SORST, JST, Sapporo 060-0810, Japan

Received July 6, 2006; Revised Manuscript Received January 27, 2007

ABSTRACT: We previously discovered that isotropic monomer solution shows birefringence due to its anisotropic structure after gelation in the presence of a small amount of rod-like polyelectrolyte. Here, we focus on what mechanism is responsible for the formation of anisotropic structure during gelation. Various optical measurements are performed to elucidate the structure change during gelation. The structure before and during gelation is in situ observed by scanning microscopic light scattering, confocal laser scanning microscope, polarizing optical microscope and depolarizing small angle light scattering. It is found that the existence of a large-size structure in monomer solution with the rod-like polyelectrolyte is essentially important to induce birefringence during gelation. The possible mechanism of the anisotropic structure formation during gelation seeded by a rod-like polyelectrolyte is proposed based on the results of these observations.

Introduction

Tissues in living organisms contain a large amount of water and are in a soft and wet gel-like state. These biological gels have a well ordered structure, which plays a crucial role in the normal functioning of the living organisms.[1−5] For example, myosin shows a liquid-crystalline (LC) structure in sarcomere, which contributes to the formation and smooth motion of muscle fibers.[4] Lipid bilayers show a phase transition between a LC state and a gel state.[5] In the LC state, the lipid bilayers allow the efficient transport of molecules. On the other hand, the synthetic gels are usually amorphous, and rarely do they possess a well-ordered structure. Thus, there have been several attempts at replicating the functionality of living organisms by introducing well-ordered structures into synthetic gels.[6−14]

In our previous work, by copolymerization of 11-(4′-cyanobiphenyloxy) undecyl acrylate (11CBA) and acrylamide (AA) monomers, poly(11CBA-*co*-AA) LC hydrogels were synthesized.[9−13] Poly(11CBA-*co*-AA) gels swollen in water display a smectic A state.[9−12] These gels show anisotropic shrinking in one direction as the temperature increases.[13] Finkelmann and co-workers have succeeded in synthesizing smectic A elastomers with uniform homeotropic orientation.[14]

Meanwhile, we have focused on synthetic polyelectrolyte poly(2,2′-disulfonyl-4,4′-benzidine terephthalamide) (PBDT).[15,16] PBDT is a unique polymer that has both rigidity and water solubility. We have reported that aqueous solution of PBDT shows nematic liquid crystalline state above a critical PBDT concentration, C_{LC}* of 2.8 wt %.[17] This concentration is quite lower than that of common lyotropic liquid crystalline macromolecules. For example, cellulose derivatives[18] generally show LC state with C_{LC}* of about 20 wt % and synthetic polyalamide, Kevlar[19] shows that with C_{LC}* of about 10 wt % in concentrated sulfuric acid. It is considered that the low C_{LC}* of PBDT is originated from its polyelectrolyte nature and its complete rigidity in structure.

In our previous paper,[20] we attempted to synthesize anisotropic gels with high water content, to mimic living organisms by template polymerization of cationic monomer *N*-[3-(*N*,*N*-dimethylamino)propyl]acrylamide methyl chloride quarternary (DMAPAA-Q) in the presence of anionic PBDT. We discovered that the gels show birefringence after gelation even at an initial PBDT concentration well below C_{LC}*. Furthermore, the gels maintain birefringence after swelling in a large amount of water.

In these gels, monomer solutions before gelation show no birefringence because initial PBDT concentration C_{LC} is lower than C_{LC}*, indicating that the monomer solutions are isotropic. However, after gelation the gels show birefringence, indicating that self-activated orientation from isotropic structure to anisotropic one occurs during gelation.

What mechanism is responsible for the formation of anisotropic structure during gelation? In this paper, various optical measurements are performed to elucidate the structure change during gelation. The structure before and during gelation is observed by scanning microscopic light scattering (SMILS), transmission electron microscope (TEM), polarizing optical microscope (POM), confocal laser scanning microscope (CLSM) and depolarizing small angle light scattering (DP−SALS). SMILS provide structural information in several nanometers to several μm. POM characterizes the orientation of molecules scale, and DP−SALS characterizes oriented domain structures in several μm to several tens of micrometers. The mechanism of the anisotropic structure formation during gelation is discussed based on the results of these observations.

Experimental

1. Sample Preparation. Synthesis of PDMAPAA-Q Gels Containing PBDT. PBDT is a water-soluble polymer with a rigid-rod-like main-chain structure. It was synthesized by an interfacial polycondensation reaction. The details of this procedure have been published previously.[16] DMAPAA-Q (Kohjin Co. Ltd.) was used as the cationic monomer without further purification. *N*,*N*′-

* Corresponding author. E-mail: gong@sci.hokudai.ac.jp.
[†] Division of Biological Sciences, Graduate School of Science, Hokkaido University.
[‡] Creative Research Initiative "SOUSEI" , Hokkaido University.
[§] School of Materials Science, Japan Advanced Institute of Science and Technology.
[||] SORST, JST.

10.1021/ma061511u CCC: $37.00
Published on Web 03/07/2007

methylenebis(acrylamide) (MBAA) (Wako Pure Chemical Industries Ltd.) was recrystallized with ethanol and used as a cross-linker. Potassium persulfate (KPS) (Wako Pure Chemical Industries Ltd.) was recrystallized with water and used as the initiator. Water was deionized and purified with 0.22 and 5 mm membrane filters before use. Aqueous solutions with a prescribed amount of PBDT, DMAPAA-Q, MBAA, and 0.1 mol % (to DMAPAA-Q) KPS were prepared. These solutions were poured into reaction cells consisting of a pair of glass plates with a 2 mm spacing. Radical polymerization was performed at 60 °C for 6 h. After gelation, the products were immersed in a large amount of water and allowed to reach an equilibrium state for a week. The swelling degree of the gels, Q, defined as the weight ratio of the sample in its swollen state to its dried state, was estimated.[21] The dried samples were obtained by keeping them in a desiccator for 12 h and in a vacuum oven at 60 °C for 6 h.

To synthesize gels with uniaxial orientation, we also performed the polymerization in high magnetic field. A direct current electromagnet, which can generate 0.4 T magnetic field, was used. The reaction cell containing 2 M DMAPAA-Q, 2 wt % PBDT, 2 mol % MBAA was put in a glass bottle capped by rubber plug with two holes punched in it. Two glass tubes were inserted into the holes, and 60 °C water was circulated in the bottle by thermostat for 6 h.

To observe PBDT distribution inside of the gels by fluorescent technique, PBDT was modified with fluoroscene molecule, fluorescein-4-isothiocyanate (FITC). FITC (Sigma-Aldrich Co.) and dimethylsulfoxide (DMSO) (Junsei Chemical Co. Ltd.) were used without further purification. A 0.2 g (0.5 wt %) sample of PBDT was dissolved in 36 mL of DMSO in a 60 °C water bath. Then 0.014 g (0.1 mol % to PBDT) of FITC dissolved in 4 mL of DMSO was added. The solution was stirred for 10 h. Then, 1 mL of water was added, and the solution was stirred for 1 h. Dried polymer was obtained by evaporating at 17 mmHg, 90 °C, and by keeping the samples in a vacuum oven at 60 °C for 4 h. This polymer was dissolved in water and reprecipitated by acetone. The precipitation was filtered and then dried in a vacuum oven at 40 °C for 4 h. This reprecipitation process was performed twice. The FITC labeled PBDT is denoted as PBDT−FITC.

We coded the samples as QP-x-y-ν, where x is the DMAPAA-Q monomer concentration in M, y is the PBDT concentration in wt %, and ν is the MBAA concentration in mol % (against DMAPAA-Q), respectively. Samples synthesized in the magnetic field are coded as QP-x-y-ν-M and FITC labeled samples are coded as QP-x-y-ν-F.

2. Structure Characterization. Observation and Measurement with Polarized Optical Microscopy (POM). Samples were placed on a glass plate and the upper free surfaces were observed by a crossed polarizing microscope (Olympus, BH-2) at room temperature. Birefringence, Δn, was measured by a crossed polarizing microscope with a Berek compensator from the retardation.[22] In the measurement, many microscopic domains randomly oriented in the bulk were observed. We chose one of large domains and selected its orientation direction by turning the sample under the crossed polarizing microscope. Δn was the average of five or six measurements at different domains for each sample.

Dynamic Light Scattering (DLS). Scanning microscopic light scattering[23−26] (SMILS) enables us to scan and measure at many different positions in the sample, in order to rigorously determine a time- and space-averaged, i.e., ensemble-averaged, (auto-)correlation function of concentration fluctuating in sample. Samples were prepared with special care to get rid of dust. A He−Ne laser (633 nm in wavelength) was used as the incident beam. The typical measuring time was 90s and scattering angles were 40, 60, 90, and 125°. The temperature of the sample was regulated at 30 °C. Scanning measurement was performed at 31 points for each sample to determine ensemble-averaged dynamic structure factor. The determined correlation function was transformed to the distribution function of relaxation time by using numerical inversed Laplace transform calculation. The same SMILS system was used for depolarized DLS, where the polarized incident beam was set vertically and the scattered light was observed horizontally with polarizer, and here we call this depolarized setting as HV and the usual setting as VV in the following. On the basis of scattering theory, the translational diffusion coefficient D is directly related to $q^2\tau_R$ as$D = 1/(q^2\tau_R)$, where q is the scattering vector and τ_R is the characteristic relaxation time at the peak of distribution function. Then, the characteristic size of diffusing objects ξ can be estimated from by using the Einstein−Stokes equation $D = k_BT/6\pi\eta\xi$, where k_B is the Boltzmann constant, T is the absolute temperature, and η is the viscosity of solvent.

Transmission Electron Microscopy (TEM) Observation. TEM observation was performed using a JEOL (JEM-1200EX) instrument at 120 kV acceleration voltage. After preparation of the sample solution, about 10 μL of the solution was dropped on carbon-coated grids (NISSHIN EM Co., Tokyo). After 3 min, 2% uranyl acetate was added to the sample, and the grids were air-dried.

Confocal Laser Scanning Microscopy (CLSM) Observation. FITC labeled samples were sliced and placed on slide glass with a 1 mm spacer, and cover glass was placed on the spacer. This sample cell was observed by CLSM (MRC-1000 UV, Bio-Rad).

In Situ Structure Analysis During Gelation. In situ observation of the gelation was performed by SMILS, crossed polarizing microscopy, and time-resolved small angle light scattering (SALS). A reaction solution containing 2 M DMAPAA-Q, 2 wt % PBDT, 2 mol % MBAA, and 0.1 mol % KPS was poured into a reaction cell consisting of a slide glass and a cover glass with a 2 mm spacing. The sample cell was placed in temperature controlled sample holder (METTLER TOLEDO, FP82HT Hot Stage) and observed by crossed polarizing microscope or measured by small angle light scattering. Gelation was performed at 60 °C. A typical SMILS measuring time was 60 s, and the scattering angle was 40°. Scanning measurement was performed at 11 points and repeated 33 times (363 min).

In the time-resolved DP−SALS measurement, we used a lab-made simple SALS system. Laser source is 5 mW He−Ne laser at 633 nm in wavelength. Scattering light was focused by converging lens and a profile was taken by CCD camera. Intensity of scattering light on concentric circle from center of profile was analyzed by image analysis software (NIH Image J).

Results and Discussion

1. Birefringence of PBDT Containing Gels. Figure 1 shows crossed polarizing microscope images of the gels synthesized at various initial PBDT concentration and MBAA concentrations at DMAPAA-Q monomer concentration $C_Q = 2$ M. All the as-prepared gels show birefringence even that PBDT concentration C_{LC} is well below C_{LC}* as shown in Figure 1a. As mentioned above, the solutions before polymerization show no birefringence because C_{LC} is well below C_{LC}*. The birefringence emerges during polymerization. The birefringence of as-prepared gels decreases with the decrease in C_{LC}. After swelling in large amount of water, all the gels still maintain birefringence as shown in Figure 1b. This is interesting because PBDT concentration in the gels, C_{LC}, decreases when the gels are swollen in water. In other words, the birefringence decreases by swelling, however, which is not directly proportional to the decrease of PBDT concentration by the swelling. When initial C_{LC} is 2 wt %, the maximum size of oriented domains is about 1 mm under the crossed polarizing microscope, as shown in Figure 1a. This size is as large as the thickness of the gel. Furthermore, the oriented domain size becomes larger after swelling.

Figure 2 shows C_{LC} calculated from the swelling degree Q as a function of cross-linker concentrationν. As ν decreases, the swelling degree Q of the gels increases and this leads to a decrease in C_{LC} in the gel. The lowest C_{LC} is only 0.004 wt %, which is 1/700 of C_{LC}*. Nevertheless, the gel still shows birefringence, as shown in Figure. 1b. This indicates that

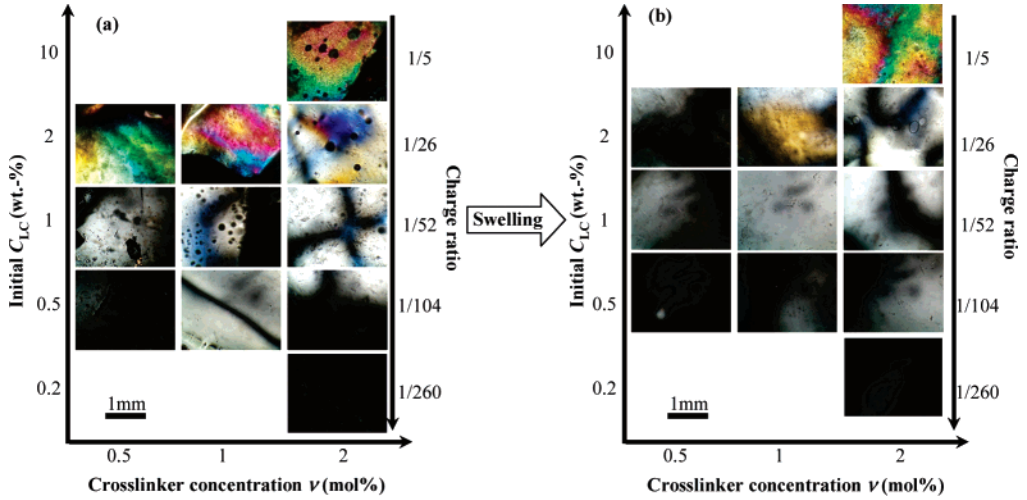

Figure 1. Polarizing optical microscopic images of the anisotropic gels synthesized at various PBDT and MBAA concentration while keeping the DMAPAA-Q concentration as constant at $C_Q = 2$ M: (a) as-prepared gels; (b) equilibrium swollen gels in water.

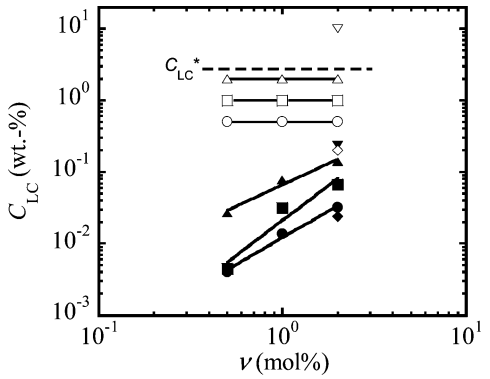

Figure 2. PBDT concentration in the gels, C_{LC}, as a function of initial cross-linker concentration ν. Open plots are C_{LC} of the as-prepared gels and closed ones are those of the equilibrium swollen gels. Broken line stands for the lower critical LC concentration of PBDT solution, C_{LC}*. C_{LC} in feed is (◇, ◆) 0.2 wt %, (○, ●) 0.5 wt %, (□, ■) 1 wt %, (△, ▲) 2 wt %, and (▽, ▼) 10 wt %. All the gels were synthesized at C_Q = 2 M.

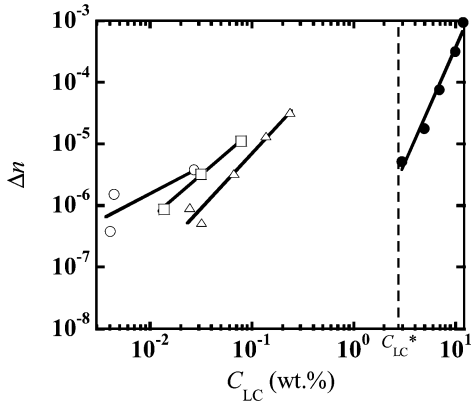

Figure 3. Birefringence, $\Delta n = n_{\parallel} - n_{\perp}$, of the anisotropic gels synthesized with various cross-linker concentration n and PBDT aqueous solutions as a function of PBDT concentration, C_{LC}. Key: (○) $\nu = 0.5$ mol %; (□) $\nu = 1$ mol %; (△) $\nu = 2$ mol %; (●) PBDT aqueous solution.

anisotropic gels can be obtained by polymerization with a very little amount of LC macromolecules as seeds.

Figure 3 shows the birefringence, $\Delta n = n_{\parallel} - n_{\perp}$, of gels and the PBDT aqueous solution. Δn of the gels is as large as that of PBDT aqueous solutions around C_{LC}*, although the values of C_{LC} of the gels are much lower than of PBDT aqueous

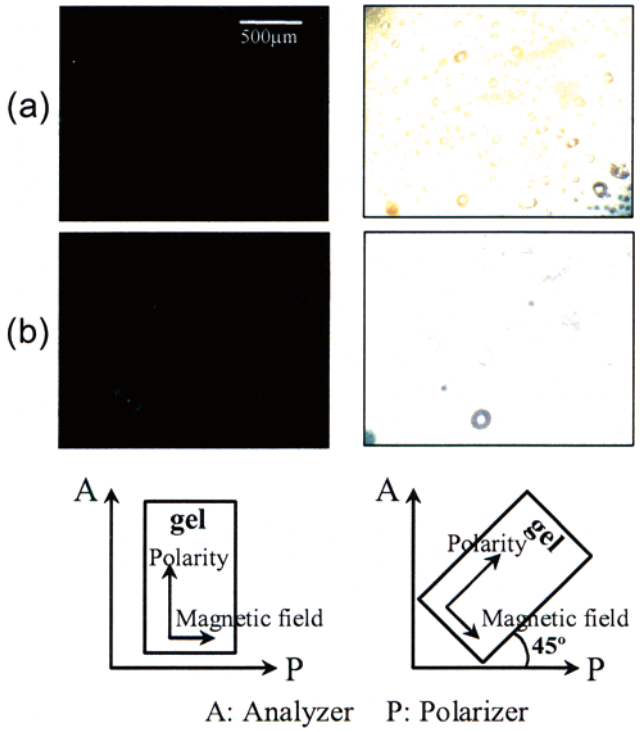

Figure 4. Polarizing optical microscopic images of the anisotropic gel, QP-2-2-2-M, synthesized under high magnetic field: (a) before swelling; (b) after swelling. The gel shows dark and bright images for every 45° rotation, indicating a uniaxial orientation structure.

solutions. This means that the large Δn of the gels is caused not only by the orientation of PBDT but also by the cooperative orientation of PDMAPAA-Q with PBDT. PDMAPAA-Q may align along PBDT, where PBDT behaves as a seed for the orientation during polymerization to form a kind of anisotropic structure. For a constant cross-linker concentrationν, Δn increases as C_{LC} increases. It is interesting to find that at the same C_{LC}, Δn increases as ν decreases. This result indicates that a loose cross-linking structure favors the anisotropic orientation of molecules.

We further tried to utilize a magnetic field to induce uniaxial orientation in the gels. Figure 4 shows polarized optical microscopic images of the gel QP-2-2-2-M synthesized under a 0.4 T magnetic field. As shown in Figure 4a, polarized optical microscopic images of the gel show dark and bright images in

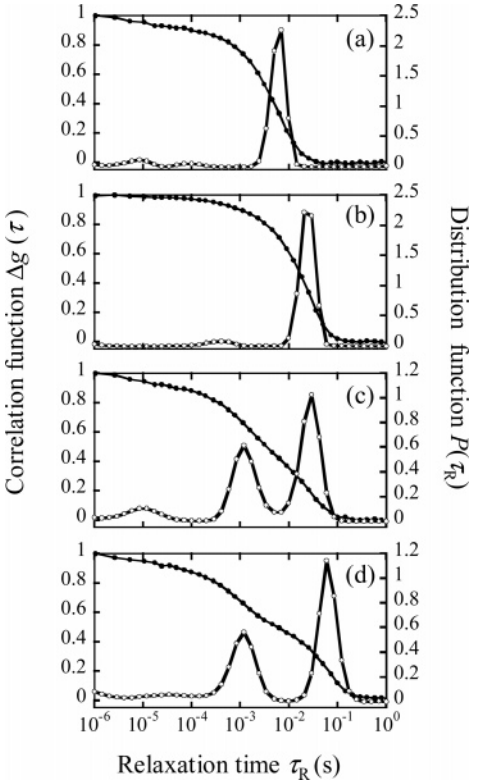

Figure 5. Correlation function, $\Delta g(\tau)$ (closed circle), and distribution function of relaxation time, $P(\tau_R)$ (open circle), of the PBDT solutions and the PBDT solutions containing DMAPAA-Q (b−d), observed by scanning microscopic light scattering at scattering angle 40°. Key: (a) QP-0-1; (b) QP-1-1; (c) QP-2-1; (d) QP-2-2.

Table 1. Correlation Length Calculated from the Distribution Function of Relaxation Time Measured by Scanning Microscopic Light Scattering

sample	peak 1 (nm)	peak 2 (nm)
QP-0-0.5	none	72
QP-0-1	none	126
QP-0-2	none	364
QP-1-1	10.4	516
QP-1-2	23.9	518
QP-2-2	23.3	1170
QP-1-1 HV	weak	395
QP-2-2 HV	very weak	none

0 and 45° directions, respectively, confirming that molecules oriented in one direction in the gel. The gel maintains this uniaxially oriented structure after swelling in water as shown in Figure 4b. A PDMAPAA-Q gel without PBDT synthesized under a magnetic field shows no birefringence.

2. In Situ Structure Analysis before and during Polymerization. The Existence of a Large Structure before Polymerization. In order to elucidate the structure formation mechanism of the present anisotropic gels, we first studied the structure of PBDT and DMAPAA-Q mixing solution before polymerization with DLS. The correlation function $\Delta g(t)$ and the distribution function of relaxation time $P(\tau_R)$ are shown in Figure 5. The DMAPAA-Q monomer solution without PBDT shows no characteristic relaxation in DLS (not shown here). However, PBDT 1 wt % solution without DMAPAA-Q monomer shows a relaxation peak at the relaxation time, τ_R, of around 10^{-2} s, as shown in Figure 5a. When DMAPAA-Q monomer is added to PBDT solution, two relaxation peaks appear as shown in Figure 5b−d. The peak of the long relaxation time is similar to that of the 1 wt % PBDT solution without DMAPAA-Q monomer as shown in Figure 5a. For all the samples,

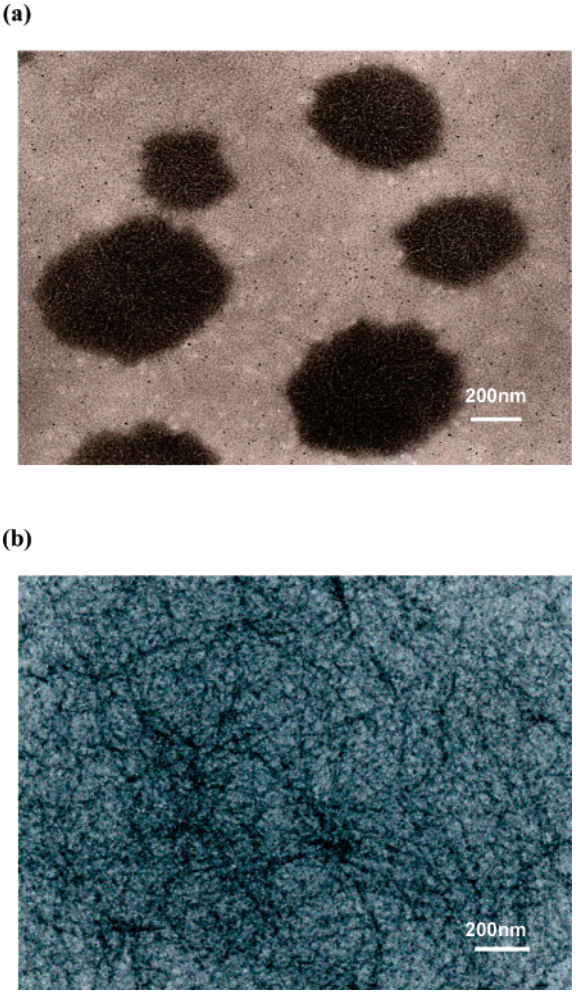

Figure 6. Transmission electron microscopic images of PBDT association, prepared by casting of the solutions: (a) QP-0-0.5 and (b) QP-1-1.

we observed the scattering-angle dependence and confirmed that all the observed relaxation modes have q^2 dependence. All the relaxation modes come from translational diffusion processes.

From the relaxation times observed by DLS, the characteristic sizes are estimated as shown in Table 1. For 0.5, 1, and 2 wt % PBDT solutions without DMAPAA-Q monomer, one relaxation peak is observed, corresponding to sizes of 72, 126, and 364 nm, respectively. Here we assume that the change in viscosity of solution is small by addition of DMAPAA-Q. Then the characteristic lengths R of structure in solution are estimated by the Stokes−Einstein formula with the viscosity of pure water at 30 °C.[23] In the case of HV observation, we also use the same estimation for translational with neglecting rotational diffusion, because the rotational component of relaxation process cannot be determined although we tried to calculate it from the scattering angle dependence of relaxation modes. The result indicates that the observed characteristic size depends on the PBDT concentration and it suggests that in the PBDT solutions rigid PBDT forms molecular association, whose size increases as the PBDT concentration. Here, the contour length of a PBDT molecule is calculated as 160 nm from the polymerization degree ($N = 100$). Thus, the characteristic size of a PBDT in solution is expected as small as several tens of nanometers, which is consistent with the observed characteristic sizes of 72−364 nm when these sizes comes from the molecular association of PBDT.

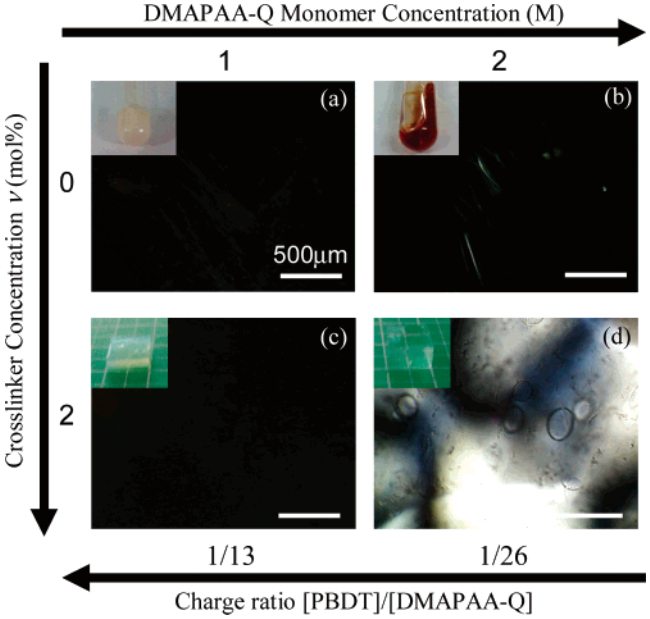

Figure 7. Polarizing optical microscopic images of the anisotropic solutions ($\nu = 0$) and gels ($\nu = 2$ mol %) synthesized at different DMAPAA-Q monomer concentration. Initial $C_{LC} = 2$ wt %. The inserted photos are the appearances of these samples. Key: (a) QP-1-2-0; (b) QP-2-2-0; (c) QP-1-2-2; (d) QP-2-2-2.

By addition of DMAPAA-Q monomer to the PBDT solution, two relaxation peaks appear. For these mixed solutions of PBDT and DMAPAA-Q, the observed characteristic sizes of the long relaxation peaks are much larger than the molecular size of PBDT. Thus, we consider that PBDT forms a large-size structure in the presence of DMAPAA-Q monomer, which is rather different from the molecular association observed in PBDT solution without DMAPAA-Q. Such a large structure is made from highly charged rigid polyelectrolytes of PBDT, which is not chemically cross-linked but physically interacted (or associated) in the presence of a large excess of counterion monomer of DMAPAA-Q to effectively screen the electrostatic repulsive force among PBDT. The small sizes of the short relaxation time is much smaller than the molecular size of PBDT, and therefore should be related to the correlation length of the inner structure in large-size structure, which corresponds to a kind of network-like structure mentioned below. It is noted that the characteristic size of the large structure becomes larger than the wavelength of incident light (532 nm) and the condition of $qR > 1$ is right, so that we observe the relatively fast relaxation mode of inner structure in large-size structures. Since the fast mode also has q^2 dependence, it can be assigned to a kind of cooperative diffusion process of network-like structure in an associated large-size structure. It means that this fast mode is different from the q^3 dependence inner-relaxation modes assigned to the Zimm model in good solvent and also different from q-independent nondiffusive relaxation mode such as subchain motion in glassy polymer system. Thus, we consider that the characteristic lengths of peak 1 in Table 1, which are estimated by the Stokes−Einstein formula, correspond to the size of network-like structure in the large-size structure of PBDT.

To confirm the light scattering results, we tried to observe the structure of molecular association by TEM. Figure 6 shows the TEM photographs of molecular association of PBDT. Figure 6a shows the particle-like aggregate of 0.5 wt % PBDT dispersed on the grid, in which rod-like fibers can be seen. It suggests that PBDT even without DMAPAA-Q monomer tends to associate. The large-sizes observed by DLS in Figure 5 are assigned to the association of PBDT. On the other hand, Figure 6b shows the network-like structure of PBDT on the grid. It suggests that PBDT also make this kind of network-like structure of the association with DMAPAA-Q monomer in solution. The short characteristic length estimated from the fast relaxation mode observed by DLS above is assigned to the mesh size of the network-like structure. Although the actual structure of PBDT association in water might be somewhat different from the TEM images, we conclude that PBDT forms a specific large structure in solution before gelation.

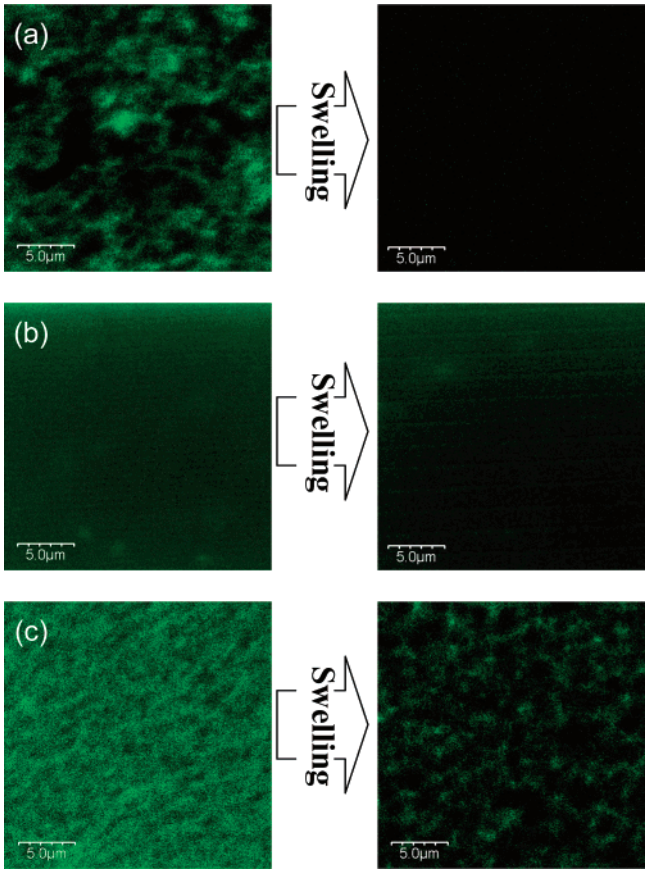

Figure 8. Confocal laser scanning microscope images of the as-prepared and swollen complex gels synthesized at different DMAPAA-Q and cross-linker concentrations. Key: (a) QP-1-1-2-F; (b) QP-2-2-2-F; (c) QP-1-1-8-F. Charge ratios of a−c are the same at 1/26.

Additionally, we perform the depolarized DLS in HV for the mixed solutions to confirm whether the relaxation modes originated from the optically anisotropic structure or not. The correlation function for HV is not shown here. As shown in Table 1, for 1 wt % PBDT and 1 M DMAPAA-Q mixed solution, the long relaxation mode is easily observed; however, the short relaxation mode is too weak to be observed. It means that the long relaxation mode comes from the optically anisotropic structure. On the basis of the above consideration, this result suggests that the large-size structure assigned by the long relaxation mode should be optically anisotropic. On the other hand, the short relaxation mode is related to an almost isotropic structure, and therefore the fast mode observed by usual DLS comes from the isotropic inner structure. For 2 wt % PBDT and 2 M DMAPAA-Q mixed solution, any obvious characteristic mode is no longer observed by depolarized DLS. It means that the optical anisotropy may diminish as the whole size of the large-size structure increases much larger than the molecular size of PBDT, where the rigidity of PBDT loses the effect of orientation induction.

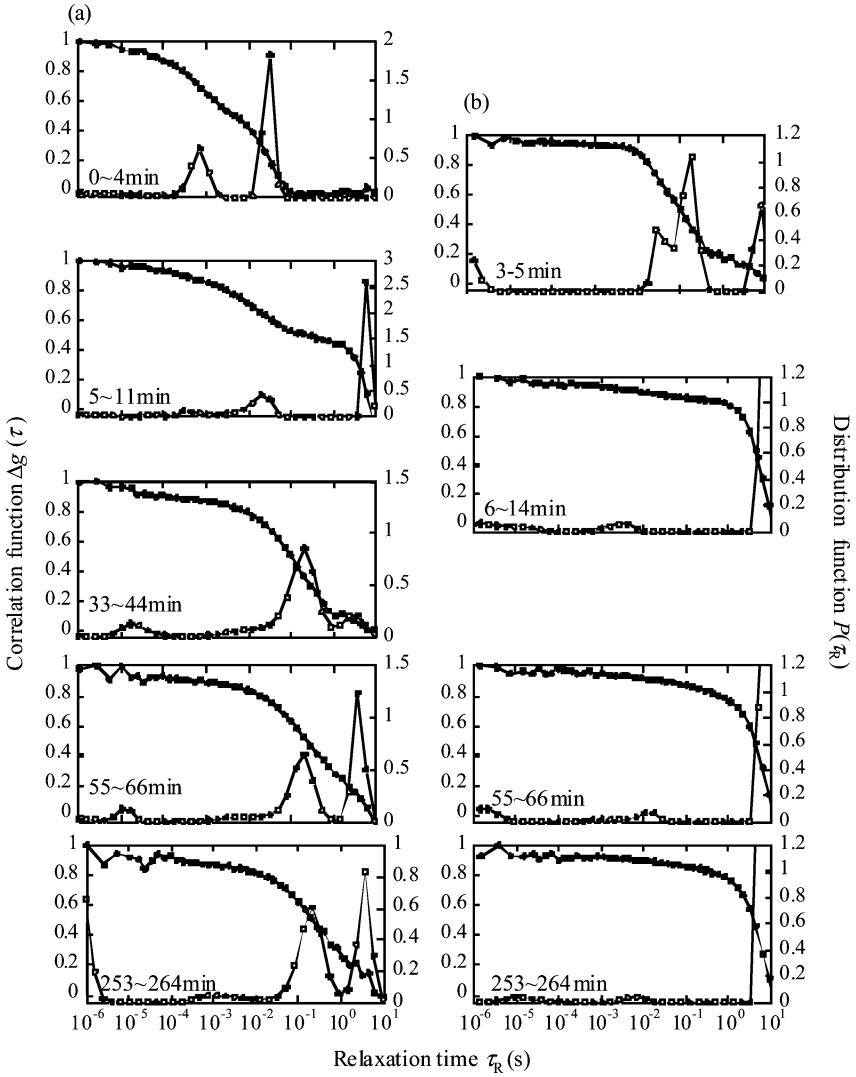

Figure 9. Correlation function, $\Delta g(\tau)$ (closed circle), and distribution function of relaxation time, $P(\tau_R)$ (open circle), observed by in situ scanning microscopic light scattering at scattering angle of 40° during gelation of QP-2-2-2. Key: (a) VV; (b) HV.

Thus, we have found that there exists a large-size structure in rod-like polyelectrolyte PBDT and cationic monomer DMAPAA-Q mixed solution even before polymerization. Here we consider the interaction between PBDT and DMAPAA-Q. The charge density of PBDT is not so dense (two anions per repeating unit of ~16 Å length) that Manning condensation does not take place. When the large amount of cationic monomer DMAPAA-Q is added to the PBDT aqueous solution, the monomer does not condense around PBDT and simply behaves as a salt, to decrease Debye screening length and weaken the repulsive force among PBDTs. This salt effect of the monomer induces the formation of large-size associated structure of PBDT. Such a structure should behave as seed for self-orientation process in the anisotropic gel formation. It is noted that this phenomenon is essentially different from usual template effect although we had called it "template polymerization" in the previous study.[20]

The Effect of Cross-Linker and Cationic Monomer on the Birefringence and Network Structure after Polymerization. Next, we focus on how the reacted solution changes after solution, depending on the presence of cross-linker and the concentration of cationic monomer. Figure 7 shows the differences in both birefringence and appearance after polymerization. In Figure 7, parts a and b, any large-size birefringence related to anisotropy in solution is not observed without a cross-linker. However, local thin birefringence of threadlike shape can be observed, which correspond to a different kind of anisotropic structure of PBDT. The appearance of solutions is transparent at high concentrations of DMAPAA-Q ($C_Q = 2$ M) in the inset of Figure 7a, but become slightly turbid at $C_Q = 1$ M in the inset of Figure 7b. It suggests that the DMAPAA-Q concentration is critical to maintain the transparency during polymerization. As shown in Figure 7, parts c and d, in the addition of the cross-linker, birefringence of samples is observed at high concentrations of DMAPAA-Q ($C_Q = 2$, 3M), but is not observed at low concentrations ($C_Q = 0.5$, 1 M) (where the results of $C_Q = 0.5$, 3M are omitted here). These results mean that both cross-linker and high concentration of cationic monomer are indispensable to the birefringence. Further, as shown in the insets of parts c and d of Figure 7, the appearance of samples is transparent at $C_Q = 2$, 3 M but becomes slightly turbid at $C_Q = 0.5$, 1 M. On the other hand, the gels prepared at $R_{PBDT} = 1$ with a small amount of DMAPAA-Q, $C_Q = 0.08$ M, become completely white, due to the formation of polyion complex. These results indicate that at high concentration of DMAPAA-Q, the large-size structure composed of PBDT and DMAPAA-Q causes a kind of disperse stability of the structure itself due to the excess amount of cationic polymer with a little amount of PBDT, which prevents the progress of phase separation, and then transparent, anisotropic gels are prepared.

This gelation process is rather different from the usual polyion-complex formation in simple mixing of polyanion and polycation, while we had called the gels "polyion-complex gels" in the previous study.[20]

To study the PBDT distribution in anisotopic gels, fluorescent-probe-attached PBDT is prepared and anisotropic gels are prepared with it. Figure 8a shows the CLSM observation of the gels. In the slightly turbid gels prepared at $C_Q = 1$ M, PBDT is distributed heterogeneously, and its characteristic size is about a few micrometers. As shown in Figure 8b, in the transparent gels prepared at $C_Q = 2$ M, the fluorescent intensity looks homogeneous. It indicates that the distribution of PBDT in the transparent, anisotropic gels is very homogeneous in several micrometer scales. On the other hand, when the cross-linker concentration increases four-times larger in the slightly turbid gels prepared at $C_Q = 1$ M, the characteristic size of heterogeneous distribution of PBDT decreases, as shown in Figure 8c Also, Figure 8c shows that the characteristic size of inner structure in polymer gels grows by swelling. On the basis of the CLSM observation, a suitable amount of cross-linker and the high concentration of counterionic monomer are important for the highly transparent but anisotropic gels by polymerization with a small amount of rod-like polyelectrolyte as seed.

In Situ Observation During Polymerization Reaction. Figure 9 shows in situ observation by DLS in both VV and HV during gelation process for QP-2-2-2. It is found that correlation function profile begins to change just after the start of reaction. The long tail of the slowest relaxation process ($>10^0$ s) in the correlation function emerges in both VV and HV, which is a characteristic sign of the formation of huge anisotropic structure due to gelation. However, its size is ranged out of the measurable window of in situ DLS in the present condition; thus, the true relaxation time of the slowest mode may slow down while the apparent relaxation time looks constant at around 10^1 s. Simultaneously, the profiles of the other peaks change as the reaction proceeds. Finally, the relaxation profile does not change after 60 min. It means that the network structure percolates at around 60 min. Apparently the fluidity of the sample is lost at 30−60 min with the tilting of the test tube and this simply observed result corresponds well to the DLS observation. Further, it should be noted that the reaction does not completely finish after the percolation. From in situ DLS observation, the formation of network structure proceeds quite quickly compared to the reaction process in the gel.

As shown in Figures 5d and 9a, there exist two relaxation modes at around 10^{-3} and $10^{-1.5}$ s in VV of DLS. As discussed above, the slower mode at around $10^{-1.5}$ s is assigned to a large-size structure and the faster mode at around 10^{-3} s is assigned to the inner structure in the large-size structure. It is noted that in HV of DLS there is no obvious relaxation mode observed before polymerization. However, just after the beginning of polymerization, the characteristic relaxation mode at around 10^{-1} s intensively appears and subsequently diminishes as the reaction progresses. It strongly suggests that the large-size structure is optically isotropic before polymerization at the present condition of QP-2-2-2, however the large-size structure becomes optically anisotropic just after the beginning of polymerization. The self-orientation process in the large-size structure should occur due to the long-range interaction induced by polymerization. Additionally, around the beginning of polymerization (<10 min), the faster mode at 10^{-3} s observed by VV is diminishing apparently, which corresponds to the decrease of the fluctuation of the network-like inner structure of PBDT in the large-size structure.

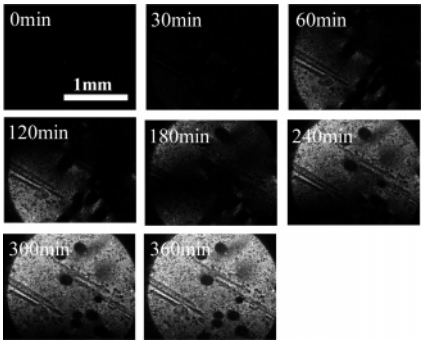

Figure 10. Crossed polarizing microscopic images at different reaction time of QP-2-2-2.

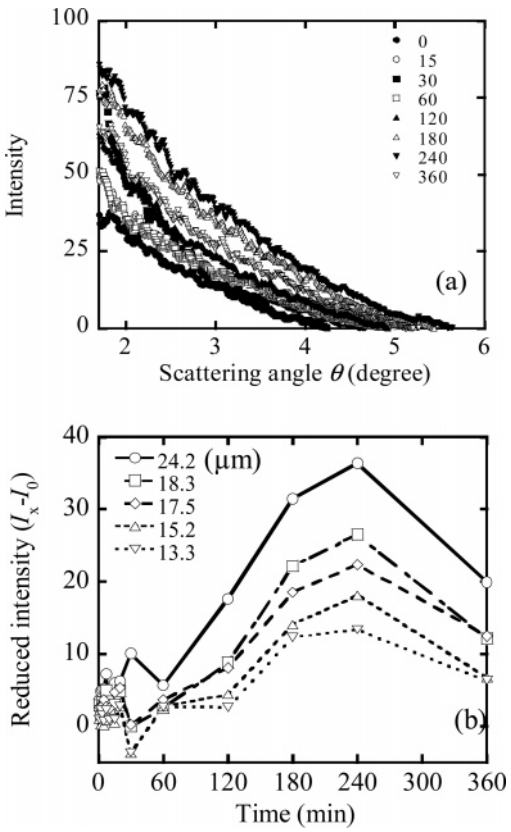

Figure 11. Depolarizing small angle light scattering during gelation of QP-2-2-2. (a) Intensity of scattering light as a function of scattering angle at various reaction times. (b) Reduced intensity, $I_x - I_0$, as a function of time for various scattering size. The numbers in part a are reaction times in minutes and in part b are characteristic size ξ in μm estimated from the scattering angles θ by the relation of $\xi = \lambda/(2n\sin(\theta/2))$.

Figure 10 shows crossed polarizing microscopic images during gelation of the sample solution of QP-2-2-2. Birefringence appears at 30−60 min and increases its intensity with the reaction time later. It means that large-scale anisotropic domain is formed when the infinite network structure is formed by the percolation, based on the in situ DLS results shown in Figure 9. The fixing of the molecular orientation to the finite network structure by cross-linkage may be crucial.

Figure 11 shows the results of in situ depolarizing small angle light scattering (DP−SALS) of the reaction solution of QP-2-2-2. Figure 11a shows the intensity of scattering light as a function of the scattering angle estimated by distance from the scattering center at various reaction times, and Figure 11b shows

the normalized intensity of scattering light as a function of reaction time for various scattering sizes. The intensity of scattering light becomes stronger after 60−120 min, indicating that oriented structure of several tens of micrometers in size increases as the reaction time proceeds, after the disappearance of the fluidity of molecule by percolation. Furthermore, the intensity of scattering light becomes less intensive 300−360 min later. This indicates that the oriented structure is disturbed by the following cross-linking reaction. It shows similar results as Figure 3 when Δn increases as ν decreases.

It should be noted that two important phenomenon are observed from the results of in situ DP−SALS. First, comparing Figure 11 with Figure 9, the reaction time is faster than the orientation time. This result indicates that inhomogeneities of the gels by phase separation and aggregation are prevented by cross-linkage because there are no characteristic lengths assigned to the phase separation or aggregate structure for QP-2-2-2. Second, the long-range correlation due to cross-linked structure is observed, which causes the long-range orientation in a large-size domain (>24 μm). Both effects can effectively contribute to the creation of the transparent and anisotropic gels with a little amount of PBDT.

We will now suggest a more detailed description of the mechanism for polymerization of anisotropic gels, as illustrated in Figure 12. Highly charged rigid anionic polyelectrolyte PBDT tends to form molecular association in water without any additional chemicals although the concentration of PBDT is lower than the critical concentration of emergence of nematic behavior C^*_{LC}. In addition of counterion cationic monomer DMAPAA-Q, PBDT forms a large-size structure like a physically cross-linked microgel. At the low concentration of DMAPAA-Q, the formed microgels have anisotropy due to the rod-like shape of PBDT. As DMAPAA-Q concentration increases, the size of the microgels becomes micrometer-scale much larger than the size of PBDT and the anisotropy diminishes due to isotropic network-like structure of several tens of nanometers. Before gelation, the microgels have little or no anisotropy and random orientation. So the pregel solution shows an amorphous (isotropic) state. When the gelation reaction starts, such microgels start to behave as seeds for self-orientation process, and large amount of cationic monomer polymerizes inside and around the microgels. The emerging excess cationic polymers with PBDT microgels form anisotropic structure, where the excess cationic polymers prevent the progress of phase separation before the percolation of gelation. Since the anisotropic structures are homogeneously cross-linked by connection to each other during gelation, the solution is gradually getting oriented enough to show birefringence as a result of formation of infinite network structure, although we have no clear idea about why the anisotropy emerges and grows during gelation. However, we think the formation of anisotropic structure with rod-like polyelectrolyte PBDT from the large-size structure existed before the start of polymerization is crucial for it. Further, both the cross-linking reaction and the excess of cationic polymer prevent macroscopic phase separation. Because of those effects, the synthesized anisotropic gels can keep their highly transparency and anisotropy, and also can maintain birefringence after swelling in a large amount of solvent. In these processes, a novel kind of anisotropic gels is synthesized from isotropic monomer solution with a quite small amount of rigid-rod macromolecule seeds.

Conclusion

By copolymerization of an excess amount of cationic monomer and cross-linker with a little amount of rod-like anionic polyelectrolyte, anisotropic gels were obtained. In these cases, the monomer solution before gelation shows no birefringence; however, the gel polymerized at high DMAPAA-Q concentration keeps transparent and show birefringence. After swollen in a large amount of water, the gels maintain birefringence even when the PBDT concentration in the gels is 1/700 of C_{LC}*. Δn of the swollen gels is as large as that of PBDT aqueous solutions above C_{LC}*, although the C_{LC} in gels is much lower than for PBDT aqueous solutions. Furthermore, it is found that the uniaxially oriented anisotropic gels are synthesized under high magnetic field. This is important for industrial application because uniaxially oriented gels will induce anisotropic properties of mechanics, transport, and so on. By using various structure characterization techniques, it is found that, for the self-orientation process during the formation of the anisotropic gels, the existence of a large-size structure formed by rigid-rod PBDT in monomer solution before gelation is crucial, which plays an important role in gelation as an effective seed growing anistropic structure. Further, the cross-linking reaction in the presence of the anisotropic structure is essentially important for this self-orientation. Such a self-orientation process by intermolecular interaction or cross-linking reaction has many analogies with the formation of well-ordered structure in living organisms, where the existence of a large-size seed may be also

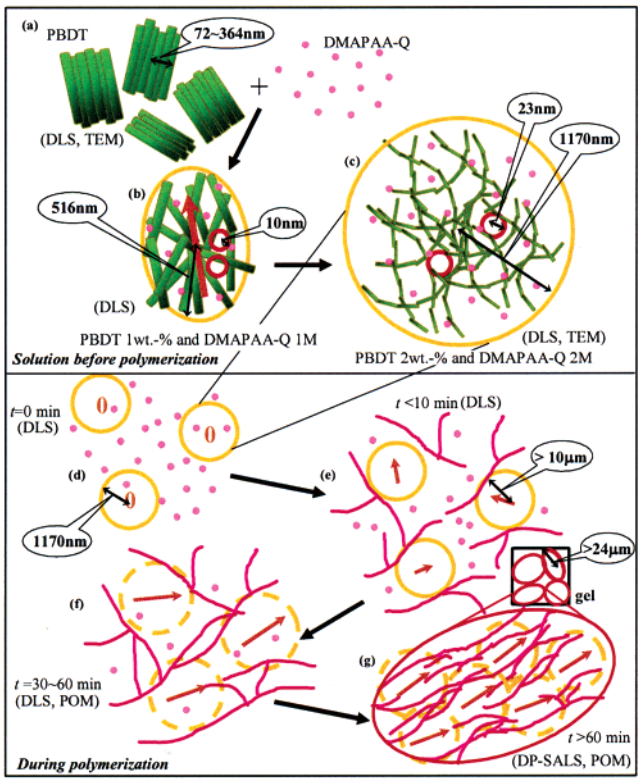

Figure 12. Illustration of the mechanism for polymerization of anisotropic gels by using a very small amount of rod-like polyelectrolyte. (a) Molecular associations of rod-like polyelectrolyte in water and counterion monomer. (b) Large-size anisotropic structure with counterion monomer, where the arrow means anisotropy and the small circles indicate mesh structure. (c) Grown network-like structure losing anisotropy. The large circle indicates the size of the structure. (d) Before polymerization. "0" in circle instead of the arrow means no anisotropy inside the large-structure. (e) Structure at the beginning of polymerization. The arrow in the circle means the emergence and growth of anisotropy. The thick line means the counterion polymer network. (f) Structure around the gelation point. Dashed line of the circle indicates the diminishing the boundary around the large-size structure and embedding in finite network of counterion polymer. (g) Final oriented domain structure in homogeneous anisotropic gels.

important similarly to the present anisotropic gels. It is possible that the role of the self-organization of rigid-rod polyelectrolyte in living organisms will be extensively revealed by clarifying the seed effect of rod-like polyelectrolyte under the formation of the oriented structure in anisotropic gels.

Acknowledgment. We would like to thank Prof. H. Orihara for his advice and help with the measurement of birefringence and thank Prof. K. Kumagai and Dr. Y. Furukawa for their advice and help with the electromagnet. We also thank Mr. K. Shikinaka for his help with TEM observation. This research was financially supported by a Grant-in-Aid for the Creative Scientific Research from the Ministry of Education, Science, Sports, and Culture of Japan.

References and Notes

(1) Evdokimov, Y. M.; Nasedkina, T. V.; Salyanov, V. I.; Badaev, N. S. *Mol. Biol.* **1996**, *30*, 219.
(2) Duvert, M.; Bouligand, Y.; Salat, C. *Tissue Cell* **1984**, *16*, 469.
(3) Spencer, M.; Fuller, W.; Wilkins, M. H. F.; Brown, G. L. *Nature (London)* **1962**, *194*, 1014.
(4) Coppin, C. M.; Leavis, P. C. *Biophys. J.* **1992**, *63*, 794.
(5) Petrache, H. I.; Gouliaev, N.; Tristram-Nagle, S.; Zhang, R.; Suter, R. M.; Nagle, J. F. *Phys. Rev. E* **1998**, *57*, 6.
(6) Hayakawa, M.; Onda, T.; Tanaka, T.; Tsujii, K. *Langmuir* **1997**, *13*, 3595.
(7) Tsujii, K.; Hayakawa, M.; Onda, T.; Tanaka, T. *Macromolecules* **1997**, *30*, 7397.
(8) Kishi, R.; Sisido, M.; Tazuke, S. *Macromolecules* **1990**, *23*, 3868.
(9) Kaneko, T.; Yamaoka, K.; Gong, J. P.; Osada, Y. *Macromolecules* **2000**, *33*, 412.
(10) Kaneko, T.; Yamaoka, K.; Gong, J. P.; Osada, Y. *Macromolecules* **2000**, *33*, 4422.
(11) Yamaoka, K.; Kaneko, T.; Gong, J. P.; Osada, Y. *Macromolecules* **2001**, *34*, 1470.
(12) Yamaoka, K.; Kaneko, T.; Gong, J. P.; Osada, Y. *Langmuir* **2003**, *19*, 8134.
(13) Kaneko, T.; Yamaoka, K.; Osada, Y.; Gong, J. P. *Macromolecules* **2004**, *37*, 5385.
(14) Nishikawa, E.; Yamamoto, J.; Yokoyama, H.; Finkelmann, H. *Macromol. Rapid Commun.* **2004**, *25*, 611.
(15) Vandenberg, E. J.; Diveley, W. R.; Filar, L. J.; Pater, S. R.; Barth, H. G. *J. Polym. Sci., Part A: Polym. Chem.* **1989**, *27*, 3745.
(16) Sarkar, N.; Kershner, L. D. *J. Appl. Polym. Sci.* **1996**, *62*, 393.
(17) Funaki, T.; Kaneko, T.; Yamaoka, K.; Ohsedo, Y.; Gong, J. P.; Osada, Y.; Shibasaki, Y.; Ueda, M. *Langmuir* **2004**, *20*, 6518.
(18) Pawlowski, W. P.; Gilbert, R. D.; Fornes, R. E.; Purrington, S. T. *J. Polym. Sci., Part B: Polym. Phys.* **1988**, *26*, 1101.
(19) Blades, H. U.S. Patent 3 869 430, 1975.
(20) Shigekura, Y.; Chen, Y. M.; Furukawa, H.; Kaneko, T.; Kaneko, D.; Osada, Y.; Gong, J. P. *Adv. Mater.* **2005**, *17*, 2695.
(21) Furukawa, H. *J. Mol. Struct.* **2000**, *554*, 11.
(22) Born, M.; Wolf, E. *Principles of Optics*, Cambridge University Press: London and Cambridge, U.K., 1959.
(23) Furukawa, H.; Horie, K.; Nozaki, R.; Okada, M. *Phys. Rev. E* **2003**, *68*, 031406.
(24) Furukawa, H.; Hirotsu, S. *J. Phys. Soc. Jpn.*, **2002**, *71*, 2873.
(25) Maestro, A.; Acharya, D. P.; Furukawa, H.; Gutiérrez, J. M.; López-Quintela, M. A.; Ishitobi, M.; Kunieda, H. *J. Phys. Chem. B*, **2004**, *108*, 14009.
(26) Naga, N.; Oda, E.; Toyota, A.; Horie, K.; Furukawa, H. *Macromol. Chem. Phys.*, **2006**, *207*, 627.

MA061511U